ZERO-SHOT RESTORATION OF UNDEREXPOSED IMAGES VIA ROBUST RETINEX DECOMPOSITION

Anqi Zhu[1], Lin Zhang[1,], Ying Shen[1,*], Yong Ma[2], Shengjie Zhao[1], Yicong Zhou[3]*

[1]School of Software Engineering, Tongji University, Shanghai, China
[2]School of Computer Information Engineering, Jiangxi Normal University, China
[3]Department of Computer and Information Science, University of Macau, Macau

ABSTRACT

Underexposed images often suffer from serious quality degradation such as poor visibility and latent noise in the dark. Most previous methods for underexposed images restoration ignore the noise and amplify it during stretching contrast. We predict the noise explicitly to achieve the goal of denoising while restoring the underexposed image. Specifically, a novel three-branch convolution neural network, namely RRDNet (short for Robust Retinex Decomposition Network), is proposed to decompose the input image into three components, illumination, reflectance and noise. As an image-specific network, RRDNet doesn't need any prior image examples or prior training. Instead, the weights of RRDNet will be updated by a zero-shot scheme of iteratively minimizing a specially designed loss function. Such a loss function is devised to evaluate the current decomposition of the test image and guide noise estimation. Experiments demonstrate that RRDNet can achieve robust correction with overall naturalness and pleasing visual quality. To make the results reproducible, the source code has been made publicly available at https://aaaaangel.github.io/RRDNet-Homepage.

Index Terms— Underexposed image restoration, Retinex decomposition, zero-shot learning

1. INTRODUCTION

Poor lighting conditions can cause serious quality degradation of captured images such as overall darkness or illegible surface details in back-lit regions. Besides, with insufficient light, the image acquired by the camera sensor usually contains latent noise. How to develop an effective and robust restorer for underexposed images remains an unresolved issue.

An important but ignored problem of underexposed image enhancement is how to suppress noise in dark areas while stretching image contrast. In classic Retinex model [1], one of the most widely-used paradigms in this field [2, 3, 4], an image I can be decomposed into illumination S and reflectance R:

$$I(\mathbf{x}) = R(\mathbf{x}) \cdot S(\mathbf{x}) \tag{1}$$

*Corresponding authors: {cslinzhang, yingshen}@tongji.edu.cn.
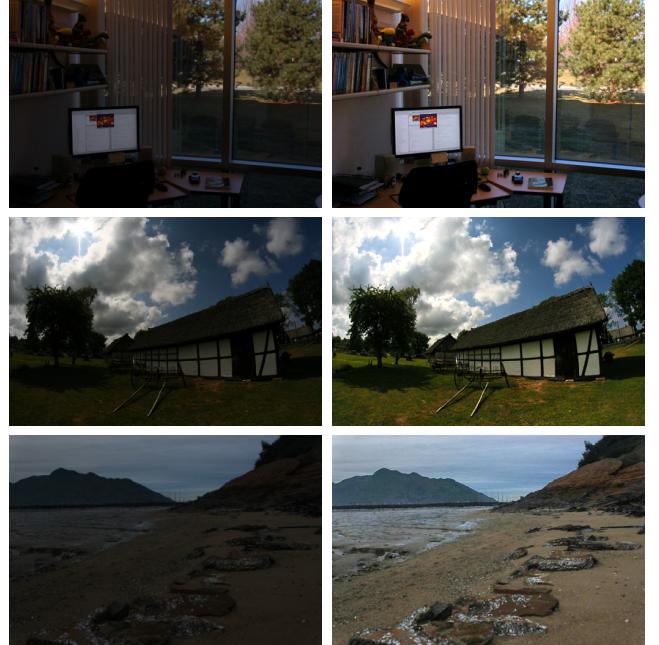
Fig. 1. Restoration results of RRDNet. Images in the left column are underexposed images in different scenes while the ones in the right column are the restored results.

where $\mathbf{x}$ denotes the spatial location of pixels. However, this classic Retinex model ignores noise, which is inevitable in underexposed images. To this end, the robust Retinex model in [5] introduces a noise term N as,

$$I(\mathbf{x}) = R(\mathbf{x}) \cdot S(\mathbf{x}) + N(\mathbf{x}) \tag{2}$$

In this work, we adopt the robust Retinex model in Eq. (2) and introduce a zero-shot scheme, namely RRDNet, to decompose the input image into three components, illumination, reflectance and noise. RRDNet is a novel three-branch CNN (Convolutional Neural Networks [6]) and can explicitly estimate the three components of the input image. After decomposition, the illumination can be adjusted and the noise can be removed, and finally, a noise-free output with high visibility is generated. Several examples are given in Fig. 1.

Most of the state-of-the-art approaches for underexposed images restoration are learning-based, but data-driven training scheme greatly limits the generalization capabilities of their models. In our scheme, RRDNet is trained while testing, implying that its weights are updated by iteratively minimizing a specially designed loss function. Such a loss function is devised to evaluate the current decomposition of the input image and ensure the quality of the restored output. Meanwhile, it can guide RRDNet to estimate the noise according to illumination distribution, thus performing denoising to avoid noise being amplified in the dark. Such a zero-shot scheme does not need any prior image examples or prior training.

2. RELATED WORK AND OUR CONTRIBUTIONS

2.1. Related work

The restoration of underexposed images has been a long-standing problem with a great progress made over the past decade. Here we divide them into two categories, plain ones and data-driven ones, based on whether or not supervised-learning is used.

Plain methods. Conventional image enhancement methods such as histogram-based methods [7, 8, 9, 10] can be explored to enhance underexposed images, but in most cases, their efficacy is quite limited. Yuan and Sun [11] proposed an automatic exposure correction method using S-curve tone mapping. Zhang *et al*. [12] designed an unsupervised scheme to estimate the best-fitting S-curve of the input. The parameterized S-curve adopted in these methods may compress the mid-tones and the output images look too flat and unnatural.

Early attempts [13, 14] based on Retinex theory remove the illumination and directly extract the reflectance as the enhanced results. Later work in this branch mainly focused on the estimation [3, 4] and adjustment [2] of illumination. These Retinex-based methods assume that the input images are noise-free and amplify the latent noise in dark regions. Fu *et al*. [15] estimated illumination and reflectance simultaneously. Li *et al*. [5] further introduced the noise term to the classic Retinex decomposition. These two methods suppress noise via imposing a constraint on the reflectance or noise. Differently, we applied the illumination guidance to noise estimation, thus performing more targeted denoising in the dark.

Data-driven methods. Black box models [16, 17, 18, 19] roughly follow such a pipeline: first collect or synthesize a dataset containing input-output pairs, and then find the mapping relationship or train an exposure correction model based on the dataset. Based on Retinex theory, Shen *et al*. [20] proposed MSR-net based on multi-scale Retinex theory and trained it on synthesized pairwise images. Wang *et al*. [21] trained an illumination mapping estimation network on the new dataset they built, including underexposed images and expert-retouched references. Wei *et al*. [22] and Zhang *et al*. [23] trained decomposition networks on a dataset containing low/normal light image pairs. The performance of these supervised-learning-based methods highly depends on the training dataset despite the fact that building such a dataset including various types of illumination and contents is a challenging task itself.

2.2. Our contributions

Using learning-based approaches is a recent trend. However, data-driven approaches have a potential drawback in their generalization capability. The latent noise in dark regions of the underexposed images is also an issue ignored by most previous methods. Our contribution is summarized as follows:

- An image-specific CNN for underexposed image restoration, namely RRDNet, is proposed. RRDNet does not require prior training; instead, it depends on internal optimization of the single input image, ensuring its generalization capability among various shooting scenes and kinds of illumination conditions.
- RRDNet has three branches, which are able to explicitly predict the illumination, reflectance and noise of the input image. This makes it possible to adjust the illumination and remove the noise completely to prevent the noise from being amplified after contrast stretching.
- In RRDNet, to optimize the decomposition of the input image, a novel loss is proposed. Such a loss can guarantee that the restored result has rich texture details. At the same time, it can guide RRDNet to focus on noise estimation in darker areas according to illumination distribution, thus performing more targeted denoising to avoid noise being amplified in the dark.
- Due to the CNN structure of RRDNet, our method could learn the representation of Retinex decomposition. With the increase of processed images, the number of iterations of RRDNet converging to the optimal decomposition decreases when facing unseen images, demonstrating the superiority of unsupervised-learning-based schemes.

3. RRDNET: A ROBUST RETINEX DECOMPOSITION NETWORK FOR UNDEREXPOSED IMAGE RESTORATION

In this section, the workflow of the proposed approach for underexposed image restoration using RRDNet will be presented in Sec. 3.1, and then in Sec. 3.2 we will introduce the details of loss function of RRDNet which is designed for zero-shot learning.

3.1. Three-branch decomposition and restoration

Given an underexposed image, the decomposition is performed according to the robust Retinex model [5]. Specifically, an underexposed image I can be decomposed into three
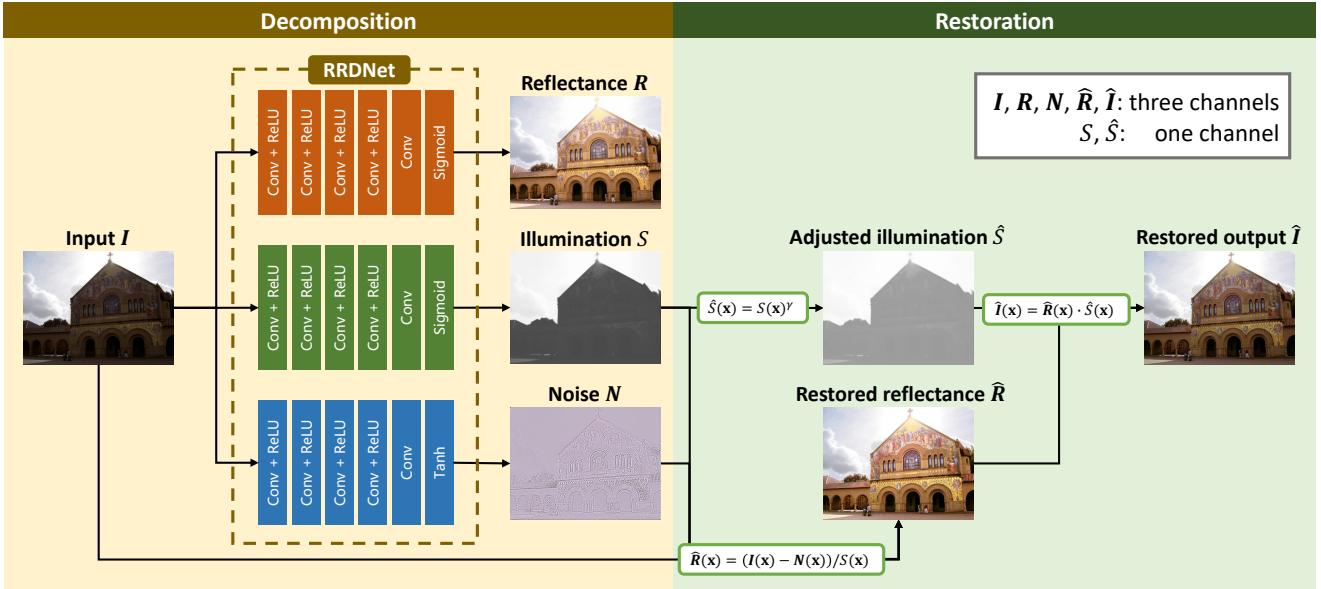
Fig. 2. The workflow of the proposed approach for underexposed image restoration using RRDNet. The three branches of RRDNet are used to estimate the reflectance, the illumination, and the noise (the noise map is normalized for visualization), respectively. Illumination map is adjusted through Gamma transformation and noise-free reflectance is computed. Combine the adjusted illumination and restored reflectance, and the restored output is generated.

components, reflectance R, illumination S and noise N as,

$$I(\mathbf{x}) = R(\mathbf{x}) \cdot S(\mathbf{x}) + N(\mathbf{x}) \qquad (3)$$

It needs to be noted that for simplicity the three color channels are usually assumed to have the same illumination [2].

Fig. 2 is the workflow of the proposed method, consisting of two stages, decomposition and restoration. In the decomposition stage, RRDNet is a three-branch fully convolutional neural network and its structure is illustrated in Fig. 2. The three branches are used to estimate the reflectance, the illumination, and the noise, respectively. The branches of reflectance and illumination end with sigmoid layer to ensure the intensities to fall in $[0, 1]$. Differently, to better fit additive noise, a tanh layer is used as the last layer of noise branch, which can make the noise value fall in $[-1, 1]$. The noise map shown in Fig. 2 is normalized for visualization. After iterations of minimizing the loss function (Details of the loss function are presented in Sec. 3.2) and updating the weights of RRDNet, final decomposition of the input image can be generated.

In the restoration stage, the illumination component is adjusted via Gamma transformation as,

$$\widehat{S}(\mathbf{x}) = S(\mathbf{x})^\gamma \qquad (4)$$

where γ is a predefined parameter. According to Eq. (3), a noise-free reflectance can be computed as,

$$\widehat{R}(\mathbf{x}) = (I(\mathbf{x}) - N(\mathbf{x})) / S(\mathbf{x}) \qquad (5)$$
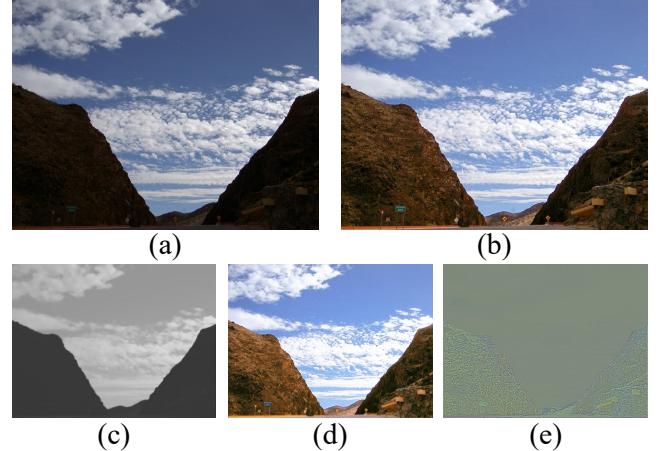
Fig. 3. The decomposition and restoration results of the RRD-Net. (a) is an input underexposed image, (c)-(e) are its estimated illumination, reflectance and normalized noise map respectively and (b) is the restoration output.

Combine the adjusted illumination and noise-free reflectance, and the final restoration result can be computed as,

$$\widehat{I}(\mathbf{x}) = \widehat{R}(\mathbf{x}) \cdot \widehat{S}(\mathbf{x}) \qquad (6)$$

3.2. Loss function for zero-shot learning

To update the weights of RRDNet, we need a loss function to evaluate the current decomposition and guide the network to

Table 1. Objective evaluation results of the competing methods.

Datasets	Yuan and Sun [11]		NPE [2]		RetinexNet [22]		Zhang et al.'s [4]		ExCNet [12]		RRDNet	
	NIQE	CPCQI	NIQE	CPCQI	NIQE	CPCQI	NIQE	CPCQI	NIQE	CPCQI	NIQE	CPCQI
MEF [24]	3.1820	0.9970	3.5469	1.0372	4.9047	0.8863	3.5223	1.1126	3.3007	1.0555	**3.1803**	**1.0981**
LIME [3]	3.7331	1.0482	3.8400	1.0812	5.1289	0.9868	4.2784	1.1415	3.7594	1.0804	**3.7763**	**1.1461**
DICM [25]	2.8680	0.7640	3.0589	0.9115	4.3084	0.8830	3.1833	0.9559	3.3656	0.9632	**2.9519**	**0.9104**
NPE [2]	3.1229	0.8125	3.2418	0.9527	4.5349	0.9125	3.4335	0.9995	3.1907	0.9490	**3.2083**	**0.9934**
Average	3.2265	0.9054	3.4219	0.9957	4.7192	0.9172	3.6044	1.0524	3.4041	1.0120	**3.2792**	**1.0370**

generate more accurate components. We design a loss function L that consists of three parts as,

$$L = L_r + \lambda_t L_t + \lambda_n L_n \tag{7}$$

where L_r, L_t and L_n are the loss components, and λ_t and λ_n are the corresponding weight factors.

Retinex reconstruction loss. The decomposed components of an image must first meet the requirements to reconstruct an image according to Eq. (3), so as to ensure the reasonable decomposition. In Retinex theory, the maximum of the R, G, B channel intensities $S_0(\mathbf{x}) = \max\limits_{c \in \{R,G,B\}} I^c(\mathbf{x})$ is usually used as an initial estimation of illumination and the reflectance is computed through the pixel-wise division between the image and its illumination map [3, 4]. Here we choose this way as a constraint on the illumination and reflectance. The Retinex reconstruction loss can be expressed as,

$$\begin{aligned} L_r = & \|\boldsymbol{I} - (\boldsymbol{R} \cdot S + \boldsymbol{N})\|_1 \\ & + \|S - S_0\|_1 + \|\boldsymbol{R} - \boldsymbol{I}/S\|_1 \end{aligned} \tag{8}$$

where $\boldsymbol{I}$ denotes the input image and the reconstructed image is computed as $(\boldsymbol{R} \cdot S + \boldsymbol{N})$. $\|\boldsymbol{X}\|_1$ computes the sum of absolute values of all the entries in $\boldsymbol{X}$. l_1-norm is used to guide the network to generate sharp illumination and reflectance.

Texture enhancement loss. In natural images, usually the illumination intensity of a surface is relatively flat. A piecewise smooth illumination map helps enhance the texture of the dark region. That is because when adjacent pixels have close intensities, their contrast will be enlarged when divided by the same illuminance value which falls in $[0, 1]$. In order to ensure that the texture is enhanced, a smoothness loss term L_t is designed as,

$$L_t = \|w_x \cdot (\partial_x S)^2\|_1 + \|w_y \cdot (\partial_y S)^2\|_1 \tag{9}$$

where x and y indicates horizontal and vertical directions. w_x and w_y are the weights to ensure the estimated map piecewise smooth. Inspired by RTV loss [26], the weight term should be inversely proportional to the gradient. Here we design the weight as,

$$w_x(\mathbf{x}) = \frac{1}{G \circ (\partial_x I_g(\mathbf{x}))^2} \tag{10}$$

where G is a Gaussian filter, $\circ$ denotes the convolution operator and I_g is the gray-scale version of the input. w_y can be computed in a similar way.

Illumination-guided noise estimation loss. In the task of underexposed image restoration, the contrast of dark region will be stretched to improve its visibility. But at the same time, the noise hiding in the dark will be amplified. Therefore, it is necessary to suppress the noise especially in the dark areas. Fortunately, the illumination map of the image has been estimated, which can be used to guide the image denoising task and can help RRDNet focus on estimating the noise in the dark through weighting. The illumination-guided noise estimation loss term is designed as,

$$L_n = \|\boldsymbol{w}_n \cdot \boldsymbol{N}\|_F + \frac{1}{\lambda_n}[\|\boldsymbol{w}_r \cdot (\partial_x \boldsymbol{R})^2\|_1 + \|\boldsymbol{w}_r \cdot (\partial_y \boldsymbol{R})^2\|_1] \tag{11}$$

where $\|\boldsymbol{X}\|_F$ means the Frobenius norm of the matrix $\boldsymbol{X}$, $\boldsymbol{w}_n$ and $\boldsymbol{w}_r$ are illumination-guided weights term and are designed as,

$$\boldsymbol{w}_n(\mathbf{x}) = \boldsymbol{I}(\mathbf{x}) \tag{12}$$

$$\boldsymbol{w}_r(\mathbf{x}) = normalize(\frac{1}{\boldsymbol{I}(\mathbf{x}) \cdot (\partial_x \boldsymbol{R}(\mathbf{x}))^2 \cdot (\partial_y \boldsymbol{R}(\mathbf{x}))^2}) \tag{13}$$

where $normalize$ denotes min-max normalization. The loss function we designed for noise estimation is based on two considerations. First, the range of values in noise map needs to be limited. Second, the noise can be suppressed by smoothing the reflectance component. Different from illumination smoothing, it focuses on points with both small horizontal and small vertical gradients, ensuring that real noise points rather than edges are smoothed. In order to estimate the noise in the dark, the above two items are weighted and restricted by the illumination map.

A decomposition example is given in Fig. 3. By combining these three loss terms, the final RRDNet can converge to decompose an image (a) into local smooth illumination map (c), noise-free and texture rich reflectance (d), and noise focused on dark area (e). (b) is the restoration result.

4. EXPERIMENTAL RESULTS

We conducted experiments to compare the performance of RRDNet with state-of-the-art approaches for underexposed image restoration quantitatively and qualitatively. Furthermore, the ablation study was performed to evaluate the impact of each component of the loss function of RRDNet.

In all experiments, we set $\gamma = 0.4$, $\lambda_t = 1$ and $\lambda_n = 5000$. The experiments were carried out on a workstation with

4

| (a) | (b) | (c) | (d) | (e) | (f) | (g) |
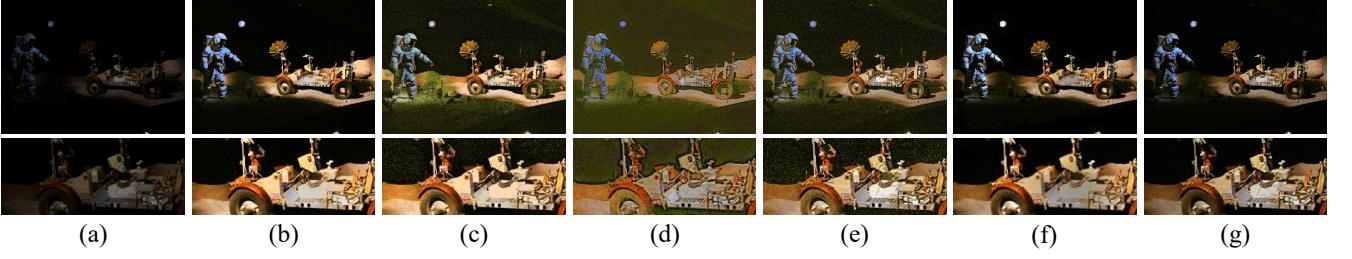
Fig. 4. Comparison on a noisy image. (a) is the input image, (b)-(g) are the results of Yuan and Sun's [11], NPE [2], 3) RetinexNet [22], Zhang et al's [4], ExCNet [12] and RRDNet.

| (a) | (b) | (c) | (d) | (e) | (f) | (g) |

Fig. 5. Comparison on an underexposed image. (a) is the input image, (b)-(g) are the results of Yuan and Sun's [11], NPE [2], 3) RetinexNet [22], Zhang *et al*'s [4], ExCNet [12] and RRDNet.

a 3.0GHz Intel Core i7-5960X CPU and an Nvidia GeForce GTX 980Ti GPU.

Datasets and compared methods. The experiments were conducted on four underexposed images datasets, including MEF [24], LIME [3], DICM [25], and NPE [2]. RRDNet was compared with five underexposed image restorers, including 1) Yuan and Sun's [11], 2) NPE [2], 3) RetinexNet [22], 4) Zhang *et al*'s [4] and 5) ExCNet [12].

Objective evaluation. Similar to [4, 5], we adopt two commonly used no reference image quality assessment metrics, NIQE (natural image quality evaluator) [27] and CPCQI (colorfulness-based patch-based contrast quality index) [28] to evaluate the underexposed image restoration methods. NIQE assesses the overall naturalness of the restored result. CPCQI evaluates the effect of enhancement between the input and enhanced output from three aspects, mean intensity, signal strength and signal structure components. A lower NIQE value roughly corresponds to a higher overall naturalness while a larger CPCQI value indicates a higher contrast.

The results over four datasets are reported in Table 1. On each dataset RRDNet can get a low NIQE value and a high CPCQI value. The performance of NPE [2], RetinexNet [22] and ExCNet [12] is inferior to RRDNet on both naturalness and contrast, especially RetinexNet. Because RetinexNet is based on supervised learning, its generalization capability deteriorates significantly on the unseen test set. Yuan and Sun's [11] method can generate results with high naturalness but the

Table 2. Ablation study.

Settings	L_c	$L_c + L_n$	$L_c + L_t$	$L_c + L_t + L_n$
CPCQI	0.8357	0.9299	1.0178	**1.0981**
NIQE	3.7438	4.1115	3.3467	**3.1803**

contrast is relatively low. Zhang *et al.*'s [4] method can generate high contrast outputs. However, since it does not suppress noise and thus the noise in the dark is amplified, the resulting images appear unnatural.

Visual Quality. Fig. 4 and Fig. 5 compare the restoration results on a noisy image and an underexposed image, respectively. (c), (d) and (e) in both Fig. 4 and Fig. 5 have serious noise in dark regions as a result of over-enhancement, which makes them appear unnatural. As for (b) and (f) in the two figures, there is a contrast distortion in their details. This is due to the S-curve adjustment model they rely on, which compresses the mid-tones and makes the texture look too flat. These observations are consistent with the objective evaluation in Table 1. By contrast, our method RRDNet can reveal the details hiding in dark regions of the image in a natural way, and at the same time obtain the high-quality output without noise artifacts.

Ablation Study. We perform an ablation study on MEF dataset to quantitatively evaluate the merit brought by each term in the loss function of RRDNet by combining different loss terms. The results are summarized in Table 2. It can be seen that adding texture enhancement loss term and

noise estimation loss term can obviously improve both contrast and naturalness of the restored outputs. The progressive improvement of the performance demonstrates the effectiveness of each loss term.

5. CONCLUSION

In this paper, we focus on underexposed image restoration and propose a zero-shot scheme, namely RRDNet to perform Retinex decomposition and restoration. RRDNet can explicitly predict the decomposition maps of the input image. The weights of RRDNet are updated by iteratively minimizing a specially designed loss function. According to the decomposed illumination, reflectance and noise components, a highly visible and noiseless output can be generated. Experiments on different datasets show the superiority of our method on both naturalness and contrast. In the future, we will further explore the adjustment methods of illumination components.

6. ACKNOWLEDGMENT

7. REFERENCES

[1] E. H. Land and J. J. McCann, "Lightness and retinex theory," *JOSA*, vol. 61, no. 1, pp. 1–11, 1971.

[2] S. Wang, J. Zheng, H.-M. Hu, and B. Li, "Naturalness preserved enhancement algorithm for non-uniform illumination images," *IEEE Trans. Image Process.*, vol. 22, no. 9, pp. 3538–3548, 2013.

[3] X. Guo, Y. Li, and H. Ling, "LIME: Low-light image enhancement via illumination map estimation," *IEEE Trans. Image Process.*, vol. 26, no. 2, pp. 982–993, 2016.

[4] Q. Zhang, G. Yuan, C. Xiao, L. Zhu, and W.-S. Zheng, "High-quality exposure correction of underexposed photos," in *MM*. ACM, 2018, pp. 582–590.

[5] M. Li, J. Liu, W. Yang, X. Sun, and Z. Guo, "Structure-revealing low-light image enhancement via robust retinex model," *IEEE Trans. Image Process.*, vol. 27, no. 6, pp. 2828–2841, 2018.

[6] Y. LeCun, Y. Bengio, and G. Hinton, "Deep learning," *Nature*, vol. 521, no. 7553, pp. 436–444, 2015.

[7] J. C. Russ, *The Image Processing Handbook*, CRC press, 2016.

[8] K. Zuiderveld, "Contrast limited adaptive histogram equalization," in *Graphics Gems IV*, 1994, pp. 474–485.

[9] C. Wang and Z. Ye, "Brightness preserving histogram equalization with maximum entropy: A variational perspective," *IEEE Trans. Consumer Electronics*, vol. 51, no. 4, pp. 1326–1334, 2005.

[10] M. Abdullah-Al-Wadud, M. H. Kabir, M. A. A. Dewan, and O. Chae, "A dynamic histogram equalization for image contrast enhancement," *IEEE Trans. Consumer Electronics*, vol. 53, no. 2, pp. 593–600, 2007.

[11] L. Yuan and J. Sun, "Automatic exposure correction of consumer photographs," in *ECCV*, 2012, pp. 771–785.

[12] L. Zhang, L. Zhang, X. Liu, Y. Shen, S. Zhang, and S. Zhao, "Zero-shot restoration of back-lit images using deep internal learning," in *MM*. ACM, 2019, pp. 1623–1631.

[13] D. J. Jobson, Z. Rahman, and G. A. Woodell, "A multiscale retinex for bridging the gap between color images and the human observation of scenes," *IEEE Trans. Image Process.*, vol. 6, no. 7, pp. 965–976, 1997.

[14] Z. Rahman, D. J. Jobson, and G. A. Woodell, "Multi-scale retinex for color image enhancement," in *ICIP*, 1996, pp. 1003–1006.

[15] X. Fu, D. Zeng, Y. Huang, X.-P. Zhang, and X. Ding, "A weighted variational model for simultaneous reflectance and illumination estimation," in *CVPR*, 2016, pp. 2782–2790.

[16] K. Dale, M. K. Johnson, K. Sunkavalli, W. Matusik, and H. Pfister, "Image restoration using online photo collections," in *ICCV*, 2009, pp. 2217–2224.

[17] V. Bychkovsky, S. Paris, E. Chan, and F. Durand, "Learning photographic global tonal adjustment with a database of input/output image pairs," in *CVPR*, 2011, pp. 97–104.

[18] Z. Yan, H. Zhang, B. Wang, S. Paris, and Y. Yu, "Automatic photo adjustment using deep neural networks," *ACM Trans. Graphics*, vol. 35, no. 2, pp. 11:1–15, 2016.

[19] F. Lv, F. Lu, J. Wu, and C. Lim, "MBLLEN: Low-light image/video enhancement using cnns.," in *BMVC*, 2018.

[20] L. Shen, Z. Yue, F. Feng, Q. Chen, S. Liu, and J. Ma, "MSR-net: Low-light image enhancement using deep convolutional network," *arXiv preprint arXiv:1711.02488*, 2017.

[21] R. Wang, Q. Zhang, C.-W. Fu, X. Shen, W.-S. Zheng, and J. Jia, "Underexposed photo enhancement using deep illumination estimation," in *CVPR*, 2019, pp. 6849–6857.

[22] C. Wei, W. Wang, W. Yang, and J. Liu, "Deep retinex decomposition for low-light enhancement," in *BMVC*, 2018.

[23] Y. Zhang, J. Zhang, and X. Guo, "Kindling the darkness: A practical low-light image enhancer," in *MM*. ACM, 2019, pp. 1632–1640.

[24] C. Lee, C. Lee, Y.-Y. Lee, and C.-S. Kim, "Power-constrained contrast enhancement for emissive displays based on histogram equalization," *IEEE Trans. Image Process.*, vol. 21, no. 1, pp. 80–93, 2011.

[25] C. Lee, C. Lee, and C.-S. Kim, "Contrast enhancement based on layered difference representation," in *ICIP*, 2012, pp. 965–968.

[26] L. Xu, Q. Yan, Y. Xia, and J. Jia, "Structure extraction from texture via relative total variation," *ACM Trans. Graphics*, vol. 31, no. 6, pp. 139:1–10, 2012.

[27] N. Hautière, J.-P. Tarel, D. Aubert, and É. Dumont, "Blind contrast enhancement assessment by gradient ratioing at visible edges," *Image Anal. & Stereology*, vol. 27, no. 2, pp. 87–95, 2011.

[28] K. Gu, D. Tao, J.-F. Qiao, and W. Lin, "Learning a no-reference quality assessment model of enhanced images with big data," *IEEE Trans. Neural Netw. Learn. Syst.*, vol. 29, no. 4, pp. 1301–1313, 2017.